Journal of the Less-Common Metals, 115 (1986) 127 - 143

CHARGE DISTRIBUTION IN SOME TERNARY ZINTL PHASES AS STUDIED BY X-RAY PHOTOELECTRON SPECTROSCOPY

HARALD PULM, GEORG HOHLNEICHER and HANS-JOACHIM FREUND*

Lehrstuhl für Theoretische Chemie, Universität zu Köln, Greinstr. 4, 5000 Köln 41 (F.R.G.)

HANS-UWE SCHUSTER, JÜRGEN DREWS and URSULA EBERZ

Institut für Anorganische Chemie, Universität zu Köln, Greinstr. 6, 5000 Köln 41 (F.R.G.)

(Received March 8, 1985)

Summary

Ternary Zintl phases MgMX (M ≡ Au, Pt, Pd; X ≡ Sn, Sb) have been studied by X-ray photoelectron and Auger spectroscopy. From an appropriate combination of binding energy and Auger kinetic energy shifts it is possible to derive an experimental estimate for the final state relaxation contributions. Inclusion of the relaxation contributions and of changes in the work function allows the determination of the atomic charges for all three constituents. The phases turn out to be much less ionic than predicted by a formal application of the extended Zintl concept. This result is in accordance with earlier suggestions derived from reflection spectroscopy.

1. Introduction

A great variety of binary and ternary intermetallic compounds show well-ordered crystallographic structures. Often the stability of these structures can be explained in the framework of a Zintl-type concept [1 - 6]. Zintl first recognized that the anion sublattice for binary compounds, which is formally obtained when an electron is transferred from the electropositive to the electronegative constituent, is isostructural to the lattice of an element with the same number of valence electrons as the electronegative constituent after electron transfer. The cations are then located in the lacunas of the anion sublattice. An extension of this concept to ternary compounds [7 - 10] leads to more complex anion sublattices which consist of two different atomic constituents.

In spite of the great success of the Zintl concept and its extensions for the prediction of stable lattice structures, the assumption of high ionicity

*Present address: Institut für Physikalische und Theoretische Chemie, Universität Erlangen-Nürnberg, Egerlandstr. 3, 8520 Erlangen, F.R.G.

0022-5088/86/$3.50

which is inherent in this model is often not in accord with the physical properties of these compounds. In many cases in which the observed crystallographic structure can be well explained by the extended Zintl concept, conductivity measurements as well as reflection spectroscopy [7, 11 - 13] indicate metallic behaviour. However, these methods probe global properties mainly determined by valence electrons. They are not particularly sensitive to the local electron distribution within the solid. Since the Zintl concept, however, is based on an assumption about the local electron distribution, it is desirable to apply spectroscopic methods that allow local properties to be probed.

High energy X-ray photoelectron spectroscopy (XPS), for example, is considered to be appropriate for such an application. Very often changes in the binding energy ΔE_B of an inner shell electron have been directly related to differences in atomic charges [14 - 19]. Such an approach neglects differential contributions to the observed binding energy shifts from the final ion states [20 - 22]. In general, however, these final state contributions have to be included: the final state carries an extra positive charge and this charge is highly localized if the electron has been removed from an inner shell. This leads to a redistribution of electrons (relaxation) in the vicinity of the hole created which in part depends on the polarizability of the surrounding atoms and the mobility of the electrons in the compound as a whole [20 - 22]. Therefore, on changing the chemical composition, the relaxation contribution changes. Consequently, in general, it is dangerous to correlate binding energy shifts with changes in atomic charges unless there is information on the relaxation contribution.

Final state effects are often evident through satellite structures accompanying the normal photoemission process [14]. Energies and intensities of such processes have been used to determine relaxation contributions [23 - 25]. However, when such processes cannot be observed different approaches have to be used. Born–Haber cycles have been designed to tackle this problem [26, 27] but sometimes these cycles rely on data, such as solution enthalpies [26, 27], that are not readily available experimentally. Wagner and coworkers have shown [28 - 31], that a combination of binding energies and Auger kinetic energies can be used to derive useful information on the final state contributions to the so called chemical shift. Recently we extended this approach by considering in detail the various hole and double-hole states involved [32]. If we want to derive an estimate for the relaxation contribution ΔR_i connected with the removal of an electron from the inner shell i, we have to combine an Auger transition (*jii*), the final state of which has two holes in i, with photoemission processes which lead to final states with holes in the shells j and i.

After having applied this method to gas-phase data of some phosphorous compounds [32] and to industrial catalysts [33] we now use this method to study the electronic structure of a group of ternary phases with the general constitution MgMX with M ≡ Au, Pt, Pd and X ≡ Sn, Sb. Formal application of the extended Zintl concept which leads to $Mg^{2+}(MX)^{2-}$ and

predicts the correct lattice, namely a filled "zinc blende-type" structure consisting of the "anions" MX with the magnesium "cations" located in the octahedral lacunas [11 - 13]. The predicted ionicity, however, is not in accordance with the metallic character indicated by reflection spectroscopy [11 - 13]. We show in this paper (Section 4) that XPS confirms the small ionicity (of the order of $Mg^{+0.5}(MX)^{-0.5}$) of the compounds, thus supporting the results derived from optical spectroscopy. In addition, our investigation yields information on the influence of different constituents M and X on the charge distribution within the "anion lattice". In Section 2 we report experimental details of the sample preparation, measurement of spectra, calibration etc., and in Section 3 we describe how to deduce atomic charges from the measured binding and Auger kinetic energy shifts.

2. Experimental details

As indicated in the introduction, combination of an Auger transition with two specific photoemission processes is necessary to obtain an experimentally derived estimate for the contribution of the final state relaxation to the binding energy shift. The processes selected for the different constituents of the Zintl phases investigated are listed in Table 1.

Photoelectron and Auger electron spectra were recorded using a modified Leybold-Heraeus LHS 10 electron spectrometer in the $\Delta E/E$ = constant mode. The energy scale was calibrated using the known binding energies of the Au $4f_{7/2}$ and Cu $2p_{3/2}$ ionizations [39]. Radiation from a silicon anode was used for the excitation. The bremsstrahlungs continuum obtained from this anode extends far enough to excite M_5 core holes in gold and platinum with sufficient probability to allow the measurement of $M_5N_{67}N_{67}$ Auger transitions in gold and platinum (E_{kin} at about 2000 eV [40]). At the same time the Si Kα line (1739.5 eV [42]) is only slightly broader than the Kα lines of magnesium or aluminium and its use does not lead to less accuracy in the determination of binding energies [33]. As an example Fig. 1 shows photoelectron and Auger spectra of the ternary compound MgAuSn and the metals magnesium, gold and tin.

The binding energies and Auger kinetic energies obtained for the metals magnesium, tin, antimony, platinum, palladium and gold are given in Table 1 together with values from the literature. The absolute binding energies agree with the literature data within a few tenth of an electronvolt. The 3d electrons of gold and platinum cannot be ionized with Si Kα radiation. It was also not possible to investigate the $L_3M_{45}M_{45}$ Auger transition of palladium, since the kinetic energy of the corresponding Auger electron does not fall in the experimentally accessible range 0 - 2000 eV.

The samples of the five available Zintl phases (MgPdSn is missing) were irregularly shaped with a diameter of about 2 mm. The samples were fixed on the sample holder by being pressed into metallic indium. This provides optimal electrical contact with the spectrometer. Charging was checked

TABLE 1

Work functions ϕ, binding energies and Auger kinetic energies for pure metals

Metal	*Process*		
		This work	*Literature value*
Mg	ϕ		3.610 [34]
	2p	49.75	49.7 [35]
	1s	1303.70	1303.0 [35]
	KL_2L_3; $^1D_2$	1185.20	1185.60 [36, 37]
Au	ϕ		5.45 [38]
	4f 7/2	83.80[a]	83.80 [39]
	3d 5/2		2205.7 [40]
	$M_5N_{67}N_{67}$	2015.85	2016 [36, 37]
Pt	ϕ		5.65 [41]
	4f 7/2	71.10	71.10 [35]
	3d 5/2		2121.1 [40]
	$M_5N_{67}N_{67}$	1960.25	1961 [36, 37]
Pd	ϕ		5.55 [41]
	3d 5/2	335.40	335.1 [35]
	2p 3/2		3173.3 [40]
	$L_3M_{45}M_{45}$		2471.0 [42]
Sn	ϕ		4.11 [43]
	4d	24.35	24.25 [35]
	3d 5/2	484.90	484.9 [35]
	$M_4N_{45}N_{45}$	436.55	437.6 [44, 45]
Sb	ϕ		4.14 [46]
	4d	32.55	32.80 [35]
	3d 5/2	528.30	528.2 [35]
	$M_4N_{45}N_{45}$	463.65	464.4 [44, 45]

The energy values given correspond to the most intense peak of the Auger multiplet.
[a]Used to calibrate spectrometer.

using previously described methods [39, 47]. No charging was found for any of the samples.

Measurements of the samples without any further treatment showed that the surfaces were covered with magnesium, antimony and tin oxides, respectively. Only in the region of the 3d ionization of antimony and tin were weak bands in addition to the oxide signals observed which could be attributed to the Zintl phases. From this we conclude that the oxide layer on the surface is only about 10 Å thick corresponding to 2 or 3 atomic layers. However, the oxide layers cause passivation, thus prohibiting further oxidation of the bulk. This observation explains quite well the "air stability" of the Zintl phases examined [11 - 13], which, from thermodynamic considerations are expected to be unstable with respect to oxidation.

As expected from earlier measurements on binary compounds, for example ref. 48, sputtering with high energy argon ions is inadequate treat-

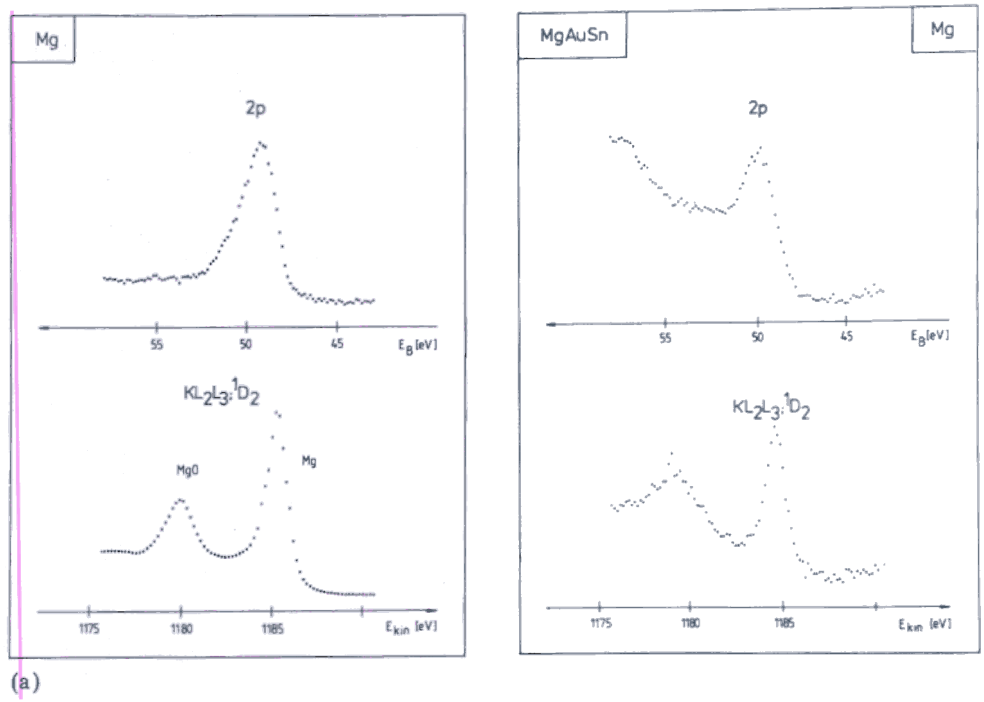

(a)

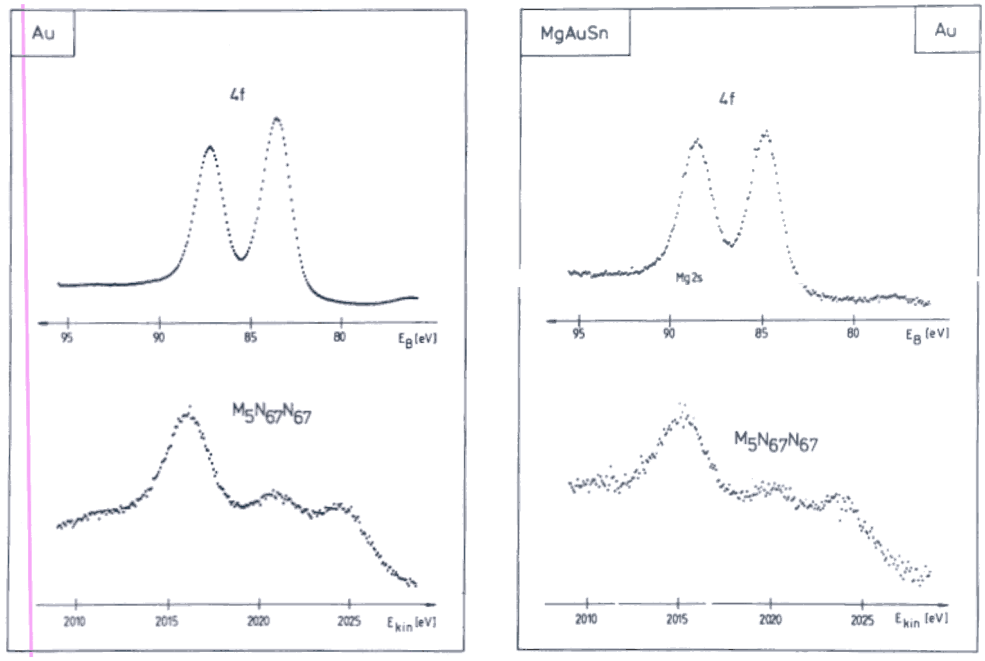

(b)

Fig. 1 ***(continued)***

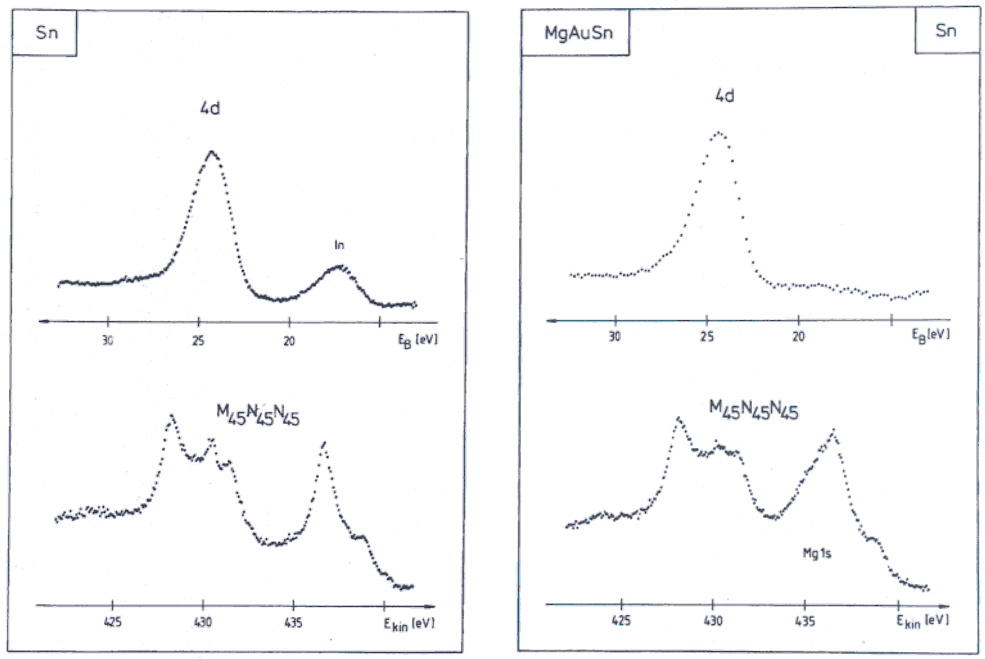

(c)

Fig. 1. Photoelectron and Auger spectra from MgAuSn and the metals (a) magnesium, (b) gold and (c) tin.

ment to obtain clean surfaces. After sputtering very little magnesium was found in the surface. Annealing at temperatures up to 150 °C did not lead to a recovery of the probed surface region. We therefore applied *in situ* cleavage under UHV conditions, as described by several authors [49 - 51]. The preparation chamber of our instrument allows us to operate with a tool perpendicular to the sample surface. Best results were obtained by using a small milling cutter. The Zintl phases are brittle and moderate pressure with the milling cutter, which did not dislocate the samples in the indium metal, led to splintering of part of the sample. The surfaces prepared by this procedure were free from oxygen. From integrated signal intensities multiplied by appropriately scaled theoretical cross sections [52] and including the energy dependence of the escape depth (see, for example, ref. 53), we obtained sample compositions, which were in accordance with the stoichiometric composition of the compounds within an error limit of 5%.

In principle the work function of a sample ϕ_s can be measured in a PE-experiment from the kinetic energy cut-off [54, 55]. Owing to the size of the sample particles, this is, however, not possible in our case. Our instrument does not allow us to illuminate a spot small enough to hit only the sample surface. Thus, the kinetic energy cut-off is always determined by the sample holder.

For the purpose of comparison we also investigated MgO, MgF_2 and $Mg(acac)_2$. The data for MgO were taken from oxidized magnesium metal. The samples of MgF_2 and $Mg(acac)_2$ were prepared by evaporation of a drop of solution deposited on a copper sample holder. In all three cases no indications of charging could be found. The data obtained for these three samples agree with literature values [56].

We investigated at least two independently prepared samples for each compound. The position of the peaks which were used to evaluate binding energy or Auger kinetic energy shifts were determined from a least-squares fit of the experimentally observed bands with a convolution of two gaussian functions. Only in the case of magnesium is the Auger multiplet split enough to specify the state ($^1D_2$) from which the Auger shift is derived. In all other cases the maximum of the Auger multiplet was used. No changes in the structure of the multiplets were observed between different samples. This latter statement is of particular importance because for the analysis we have to assume that the character of the double-hole state is the same for all samples.

The measured shifts are collected in Tables 2 - 4. We have included in Table 2 data from the literature for two binary magnesium phases: Mg_3Au crystallizes in the hexagonal Na_3As-type structure which is the hexagonal analogue of the cubic blende-type lattice [57, 58]. Mg_2Cu crystallizes in a complicated face-centred orthorhombic structure [57, 58]. The shifts derived from our own measurements all refer to our own data for the pure metals to avoid any influence of possible errors in the absolute binding energy scale. In most cases the metal was measured before and after the other samples to exclude drifts in the ramp voltage of the spectrometer.

TABLE 2

Binding energy ΔE_B and Auger kinetic energy $\Delta E(\mathrm{Aug})$ shifts for magnesium

	$\Delta E_B(1s)$	$\Delta E_B(2p)$	$\Delta E(\mathrm{Aug})$	$\Delta \bar{E}_B$	ΔR	$\Delta R'$	$-(\Delta E_B(2p) + \Delta R)$
MgAuSn	0.35	0.40	−0.60	0.45	−0.075	−0.10	−0.325
MgAuSb	0.70	0.35	−0.90	0.00	−0.45	−0.275	0.10
MgPtSn	0.40	0.30	−0.35	0.20	−0.075	−0.026	−0.225
MgPtSb	0.50	0.35	−0.50	0.20	−0.15	−0.075	−0.20
MgPdSb	0.50	0.35	−0.55	0.20	−0.175	−0.10	−0.175
Mg_2Cu	0.10	0.40	−0.20	0.70	0.25	0.10	−0.65
Mg_3Au	0.20	0.30	−0.45	0.40	−0.025	−0.075	−0.275
$Mg(acac)_2$	0.9	0.0	−4.5	−0.9	−2.7	−2.25	2.7
MgO	2.5	1.8	−5.2	1.1	−2.05	−1.7	0.25
MgF_2	1.9	0.8	−7.0	−0.3	−3.65	−3.1	2.85

$\Delta \bar{E}_B$, after eqn. (5); ΔR and $\Delta R'$, relaxation contributions from eqn. (5) and eqn. (7) respectively.

TABLE 3

Binding energy ΔE_B and Auger kinetic energy ΔE(Aug) shifts in tin and antimony

	ΔE_B(3d)	ΔE_B(4d)	ΔE(Aug)	$\Delta \bar{E}_B$[a]	ΔR[a]	$\Delta R'$[a]	$-(\Delta E_B(4d) + \Delta R)$
MgAuSn	0.05	0.15	−0.10	0.25	0.075	0.025	−0.225
MgAuSb	−0.20	−0.25	0.10	−0.30	−0.10	−0.075	0.35
MgPtSn	0.05	−0.05	−0.50	−0.15	−0.325	−0.275	0.375
MgPtSb	0.0	−0.05	−0.15	−0.10	−0.125	−0.10	0.175
MgPdSb	−0.25	−0.10	0.05	0.05	0.05	−0.025	0.05

[a] See footnote to Table 2.

TABLE 4

Binding energy ΔE_B and Auger kinetic energy ΔE(Aug) shifts for gold and platinum

	ΔE_B(4f)	ΔE(Aug)	$\Delta R'$[a]	$-(\Delta E_B + \Delta R)$
MgAuSn	1.05	−0.75	0.15	−1.20
MgAuSb	0.75	−0.75	0.00	−0.75
MgPtSn	0.25	−1.15	−0.45	0.20
MgPtSb	0.30	−1.20	−0.45	0.15

[a] See footnote to Table 2.

3. Evaluation of atomic charges

In photoemission one studies transitions from the ground state of an N-electron system (the initial state) to the ground state and to excited states of an $(N-1)$-electron system (the final state). Usually the final states of the most intense transitions can be described as "hole states" where an electron is removed from a valence or an inner shell orbital [15, 20 - 22, 59 - 61]. In the case of intense satellite structure the situation is somewhat different [23 - 25]. For final states which are hole states the binding energy can be expressed as

$$E_B(i) = -\epsilon_i - R_i - \phi_s \quad (1)$$

ϵ_i is the orbital energy of the orbital from which the electron is removed. R_i is the "relaxation energy" [20 - 22, 61], an energy contribution which results from the adjustment of the screening electrons to the creation of a hole in the ith orbital. For solids the work function ϕ_s of the sample has to be subtracted on the right-hand side of eqn. (1), since our binding energies refer to the Fermi level and not to the vacuum level [35]. Consequently for the shift in binding energy we have

$$\Delta E_B(i) = -\Delta\epsilon_i - \Delta R_i - \Delta\phi_s \quad (2)$$

In the case of the inner shell orbitals being well localized at a certain atom, changes in orbital energies $\Delta\epsilon_i$ can be related to atomic charges via potential models [16, 19, 62]. These models are quite successful, especially when we relate changes in orbital energies to changes in atomic charges. In its most common form this relation is given by

$$\Delta\epsilon_i = k'_{A,i}\Delta q_A + \Delta V(q_B) \tag{3}$$

where A denotes the atom in which the inner shell orbital i is located; q_A is the charge on atom A; V is the electrostatic potential acting at the location of atom A caused by the charges on the other atoms q_B and $k'_{A,i}$ is a parameter specific to the atom and the orbital. Often an even simpler relation is used in which only q_A is considered [16, 19, 62]:

$$\Delta\epsilon_i = k_{A,i}\Delta q_A \tag{4}$$

As shown recently [32] we can evaluate ΔR from

$$\begin{aligned}\Delta R_i &= \Delta\alpha(jii, i) - \tfrac{1}{2}\Delta\alpha(jii, j) \\ &= \tfrac{1}{2}\{2\,\Delta E_B(i) - \Delta E_B(j) + \Delta E_{kin}(jii, X)\} \\ &= \tfrac{1}{2}\{\Delta\bar{E}_B(i, j) + \Delta E_{kin}(jii, X)\}\end{aligned} \tag{5}$$

α is the "Auger parameter" introduced by Wagner [28 - 31]. It is defined as the sum of a binding energy and an Auger kinetic energy:

$$\alpha(jkl, X; i) = E_B(i) + E_{kin}(jkl, X) \tag{6}$$

X defines a special state within the Auger multiplet, but since we assume the multiplet to shift as a whole we can suppress X when we deal only with shifts of the Auger parameter. As long as $E_B(i)$ and $E_{kin}(jkl, X)$ are obtained from the same sample under the same experimental conditions α does not depend on the work function ϕ and it is not influenced by sample charging [28 - 31].

To determine ΔR_i from eqn. (5), we have to combine the following three processes:

(i) an Auger transition *jii*, the final state of which has two holes in orbital i;

(ii) the photoemission by which an electron is removed from orbital i;

(iii) the photoemission by which an electron is removed from orbital j, the orbital carrying the hole in the initial state of the Auger transition.

The main approximation inherent in the derivation of eqn. (5) (see Appendix for details) is the assumption that the relaxation results mainly from coulomb contributions [32]. If the holes are in the same orbital, the relaxation energy of the double-hole final state of the Auger transition is then four times as large as the relaxation energy of the single-hole final state of the photoemission process. The condition really needed for the applicability of eqn. (5) is even weaker, since only that part of the relaxation energy that changes with changes in the chemical environment has to be of coulomb type.

The ΔR obtained from the measured ΔE_B and ΔE_{kin} values are listed in Tables 2 and 3. Since the 3d binding energies of platinum and gold were not accessible experimentally, we do not know $\Delta\alpha(jii, j)$. Instead of eqn. (5) we therefore have to use the cruder approximation [28 - 32]

$$\Delta R'_i = -\tfrac{1}{2}\Delta\alpha(jii, i) \tag{7}$$

for these elements (Table 4). To test how much the use of eqn. (7) instead of eqn. (5) influences the final results, we also evaluated $\Delta R'$ for magnesium (Table 2) and the two metalloids tin and antimony (Table 3).

As mentioned in Section 2 we were not able to determine the work functions ϕ_s for the Zintl phases. Even with the knowledge of ΔR and $\Delta R'$, it is therefore not possible to evaluate the $\Delta\epsilon$ directly from eqn. (4). To circumvent this problem we applied the "relaxed potential model" proposed by Wertheim *et al.* [63]. In this model the binding energy shifts are calculated in a point charge approximation but final state relaxation and changes in the Fermi energy ϵ_F are included

$$\Delta E_B(i) = F_{i,\,val}\,\Delta q_A - M\,\Delta q_A - \Delta R_i + \Delta\epsilon_F \tag{8}$$

where q_A is again the charge at the atom being considered, $F_{i,\,val}$ describes the coulomb interaction between the core orbital i and the valence orbitals and M is the Madelung potential at the location of atom A.

The F integrals have been tabulated by Mann [64]. The values for the integrals needed here are listed in Table 5. The integrals have been calculated for free atoms. Since the nearest-neighbour distances d_{AB} in solids are usually smaller than the sum of the atomic radii $R_A + R_B$, we have scaled the tabulated integrals by $2R_A/d_{AA}$, where d_{AA} is the nearest-neighbour distance in the corresponding metal. This procedure seems adequate to take compression [65] into account as the F integrals are strongly related to the expectation values of $1/r$ [65]. The scaled values are included in Table 5.

We followed the procedure proposed in references [65] and [66] for the Madelung potentials: a Watson sphere of unit charge and radius $d_{AA}/2$ is used to calculate these potentials. The values obtained are shown in Table 5.

TABLE 5

Integrals $F(i, j)$ and Madelung potentials M used in connection with the evaluation of atomic charges

A	(i, j)	$F(i, j)$	F_{scal}	M	$k_{iA} = M - F_{scal}$
Mg	(2p, 3s)	10.12	10.92	9.03	−1.89
Au	(4f, 6s)	8.90	12.10	10.01	−2.09
Pt	(4f, 6s)	8.75	12.56	10.40	−2.16
Sn	(4d, 5p)	9.65	11.11	9.54	−1.57
Sb	(4d, 5p)	10.68	11.63	10.03	−1.60

[a] From ref. 64.

Equating changes in the Fermi energy $\Delta\epsilon_F$ with negative changes in the work function finally leads to

$$\Delta E_B(i) = (F_{i,\,val} - M)\,\Delta q_A - \Delta R_i - \Delta\phi \qquad (9)$$

From comparison with eqns. (3) and (4) it is obvious that $(F_{i,\,val} - M)$ is a theoretical estimate for the parameter $k_{A,\,i}$ defined in eqn. (4). The k values obtained from the scaled F integrals and the calculated Madelung potentials are given in the last column of Table 5.

For a ternary compound three equations of the above type are available: one for each constituent. The three $\Delta\phi$ appearing in the three equations contain only a single unknown — the work function ϕ_s of the sample — since the work function of the metals, which were used as reference compounds, are known (Table 1). From the three eqns. (9) and from the electroneutrality condition

$$\sum \Delta q_A = 0$$

we can therefore calculate the three Δq_A and ϕ_s.

For the Zintl phases where we have experimental data for all three constituents, the atomic charges and the work functions obtained from this procedure are shown in Table 6. Two sets of data are presented. The first set, denoted I, is based on the ΔR values of Tables 2 and 3 and the $\Delta R'$ values of Table 4. The second set, denoted II, is based on the $\Delta R'$ values of all three constituents.

TABLE 6

Work functions ϕ_s and atomic charges q derived for four ternary Zintl phases

MgMX		ϕ_s	q_{Mg}	q_M	q_X
MgAuSn	I	3.78	0.27	−0.20	−0.07
	II	3.81	0.27	−0.19	−0.08
MgAuSb	I	4.28	0.30	−0.18	−0.13
	II	4.22	0.36	−0.21	−0.16
MgPtSn	I	4.52	0.60	−0.62	0.02
	II	4.48	0.61	−0.63	0.02
MgPtSb	I	4.45	0.55	−0.63	0.08
	II	4.41	0.57	−0.64	0.07

Data sets I and II are derived using different approximations (see text).

4. Discussion

The data for magnesium are plotted in Fig. 2 in a form similar to the "chemical state" plots introduced by Wagner [28 - 31]. The difference is that

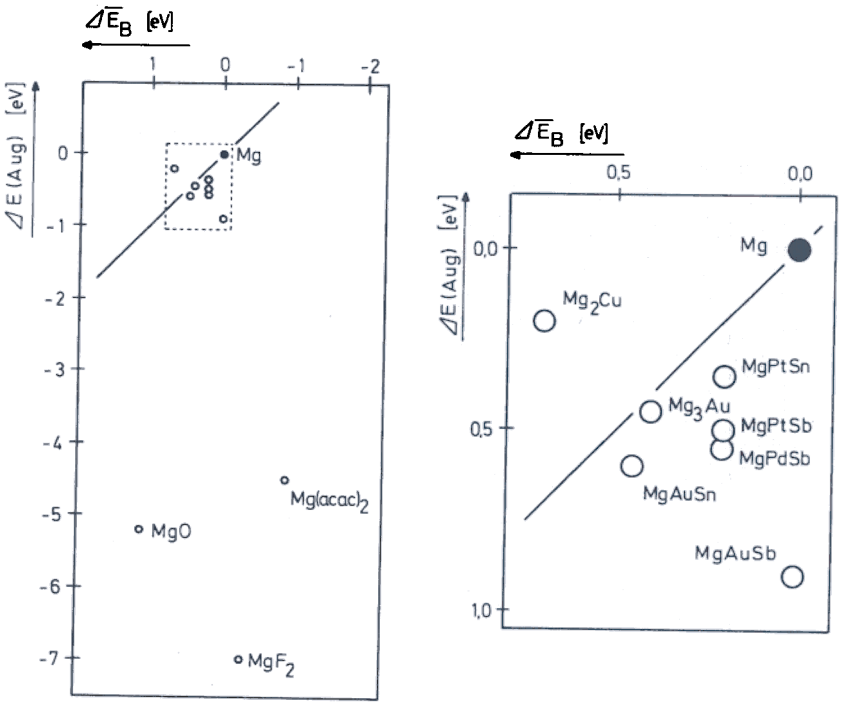

Fig. 2. Modified chemical state plot for magnesium.

we plot $\bar{E}_B(i,j) = 2E_B(i) - E_B(j)$ on the abscissa instead of $E_B(i)$ as in the conventional chemical state plot. The vertical distance to the 45°-line indicated corresponds to twice the relaxation contribution ΔR (cf. eqn. (5)). For all compounds except one (Mg_2Cu) ΔR is negative. It is strongly negative for compounds like MgO, MgF_2 and $Mg(acac)_2$. This is exactly what is expected. In the metal the mobile electrons screen a localized positive charge most efficiently. In an insulator like MgO or MgF_2 the screening can be due only to a polarization of the surrounding atoms, a process certainly less efficient than metallic screening. Similar results to those for magnesium are found for the other constituents of the ternary phases. The changes in relaxation energy with respect to the metal are negative or only slightly positive. Altogether, the changes in relaxation are quite small for the Zintl phases investigated compared with the "ionic" compounds which gives a first indication that the phases are basically metallic.

Let us try to construct a $\Delta\epsilon_i$ diagram by eliminating the contributions ΔR_i and $\Delta\phi$. We have drawn the measured ΔE_B(Mg) in Fig. 3(a) in the form of a "level diagram". If one stopped at this point and related the 2p binding energy shifts directly to variations in 2p orbital energy one would conclude that the charge on magnesium is nearly the same in all the intermetallic compounds investigated, irrespectively of the specific constituents. Even more intriguing, magnesium in the acetylacetonate would appear neutral in such a treatment and MgF_2 only half as ionic as MgO. These inconsistencies

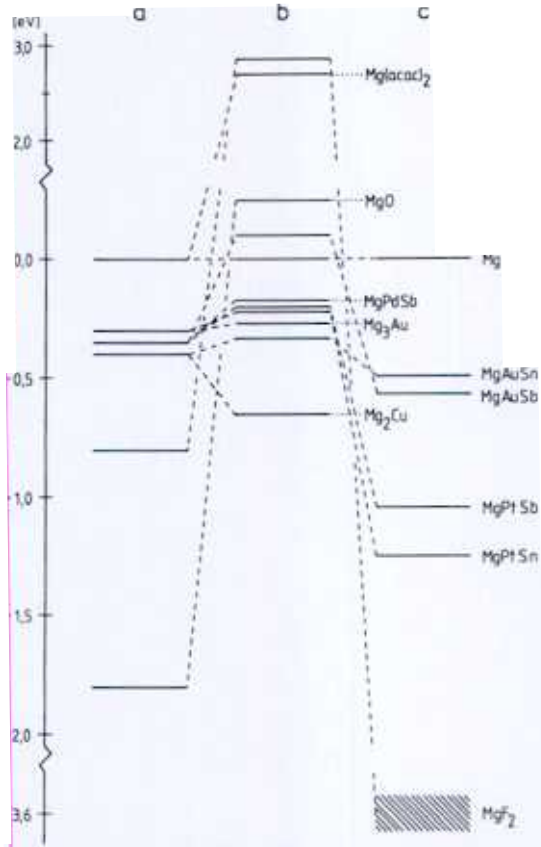

Fig. 3. Level diagram for Mg 2p: (a) based on binding energies, (b) final-state relaxation included and (c) relaxation and changes in work function included. Magnesium metal is used as the reference in all three cases.

are surely due to the neglect of ΔR and $\Delta\phi$. Even for the intermetallic compounds where we found ΔR to be relatively small, ΔR is of the same order of magnitude as ΔE_B. In Fig. 3(b) we show $-(\Delta E_B + \Delta R)$. The large differences in ΔR between intermetallic and "ionic" compounds become obvious in this presentation. However, Fig. 3(b) is also not a good approximation to a $\Delta\epsilon_i$ diagram. To derive the latter we have to take $\Delta\phi$ into account (see eqn. (4)). At present this is only possible for the four Zintl phases where we could investigate all three constituents. With the work functions given in Table 6 (data set I), we finally obtain Fig. 3(c) which can be considered as an experimentally derived approximation to an orbital diagram. Unfortunately we cannot include the "ionic" compounds in Fig. 3(c), since we have no information on $\Delta\phi$. For insulators one can only use values of ϕ_s obtained together with the other data, as the position of the actual Fermi level within the band gap depends on the measuring conditions [59]. A rough estimate of ϕ_s, however, using the method described by

Nethercot [67] yields about 10 eV for MgF_2 and therefore $\Delta\phi \approx 6$ eV, a value which brings the MgF_2 level at least in the proper range. From k_{Mg2p} given in Table 5 we obtain $\Delta\epsilon = -3.8$ eV if magnesium is really Mg^{2+} in MgF_2.

The atomic charges (Table 6) calculated using the two different approximations for the relaxation contribution are nearly the same. Only in the case of MgAuSb are the differences somewhat larger but the trends indicated are unchanged. We are therefore quite confident that the use of $\Delta R'$ instead of ΔR for gold and platinum has little influence on the general structure of our results.

First of all we find little ionicity as suggested by the small relaxation contributions. The positive charge on magnesium and correspondingly the negative charge on the "anion lattice" is about 0.3 for the gold-containing phases and about 0.6 for the platinum-containing phases. This is only about one quarter the charge predicted by a formal application of the Zintl concept. The fact that the charge separation is about twice as large in the platinum-containing phase as in the gold-containing phases can be attributed to the fact that platinum, with its ground state configuration $5d^96s^1$, is better suited to stabilize negative charge than is gold, with the ground state configuration $5d^{10}6s^1$. In this context it would be highly desirable to include the palladium-containing phases and possibly also silver-containing phases in this investigation. To do so, the technical problems mentioned in Section 2 have to be solved.

The relatively small charge separation found for the compounds studied to date is in accord with the metallic character indicated by reflection spectroscopy [12, 13]. The metallic character is also supported by the fact that these compounds show a certain homogeneity range which is not observed for highly ionic systems.

Closer inspection of the charge distribution within the anion lattice confirms the above conclusions. In the case of gold the metalloid (tin or antimony) has to participate in the stabilization of the negative charge. For platinum the metalloid is neutral or slightly positive. We do not find systematic differences between tin and antimony which is in accordance with the nearly equal electronegativity of these two elements (Sn, 1.7; Sb, 1.8 on the Allred–Rochow scale [68]). The number of examples that we have studied in detail as yet is certainly too small to draw more general conclusions on the role of the metalloid X. The examples studied so far seem to show that the charge distribution in ternary Zintl phases of the type MgMX is governed mainly by the nature of M.

To extend our understanding of the charge distribution in intermetallic compounds and of the interplay between donor and acceptor qualities of the constituents, we are currently studying intermetallic compounds which are expected to be more "ionic", in the sense that they show a more distinct charge separation between formal anions and cations. These compounds have electrovalent compositions and are semiconductors without any homogeneity range.

Acknowledgments

The authors thank the Deutsche Forschungsgemeinschaft and the Fonds der Chemischen Industrie for financial support. Part of the work was supported from the Schwerpunkprogramm "Hochenergetische Spektroskopie elektronischer Zustände in Festkörpern und Molekülen".

References

1 F. Laves, *Naturwissenschaften, 29* (1941) 241.
2 E. Zintl, *Angew. Chem., 52* (1939) 1.
3 E. Busman, *Z. Anorg. Allg. Chem., 313* (1961) 90.
4 W. Klemm and E. Busman, *Z. Anorg. Allg. Chem., 319* (1963) 297.
5 H. Schäfer, B. Eisenmann and W. Müller, *Angew. Chem., 85* (1973) 742.
6 H. Pauly, A. Weiss and H. Witte, *Z. Metallkde., 59* (1968) 47.
7 H.-U. Schuster, *Z. Anorg. Allg. Chem., 370* (1969) 149.
8 H.-U. Schuster, D. Thiedemann and H. Schönemann, *Z. Anorg. Allg. Chem., 370* (1969) 160.
9 W. Bockelmann and H.-U. Schuster, *Z. Anorg. Allg. Chem., 410* (1974) 241.
10 G. Schroeder and H.-U. Schuster, *Z. Naturforsch., 30b* (1975) 978.
11 U. Eberz, W. Seelentag and H.-U. Schuster, *Z. Naturforsch., 35b* (1980) 1341.
12 A. von Petersenn, *Dissertation,* Universität zu Köln, 1981.
13 U. Eberz, *Dissertation,* Universität zu Köln, 1983.
14 K. Siegbahn, C. Nordling, G. Johansson, J. Hedman, P. F. Heden, K. Hamrin, U. Gelius, T. Bergmark, L. O. Werme, R. Manne and Y. Baer, *ESCA Applied To Free Molecules,* Elsevier, Amsterdam, 1971.
15 K. Siegbahn, C. Nordling, A. Fahlman, R. Nordberg, K. Hamrin, J. Hedman, G. Johansson, T. Bergmark, S.-E. Karlson, I. Lindgren and B. Lindgren, *Nova Acta R. Soc. Sci. Ups. Ser. 4,* (1967) 20.
16 U. Gelius, *Phys. Scr., 9* (1974) 133.
17 M. E. Schwarz, in D. A. Shirley (ed.), *Electron Spectroscopy,* Elsevier, Amsterdam, 1972.
18 M. E. Schwarz, *Chem. Phys. Lett., 6* (1971) 631.
19 H. Basch, *Chem. Phys. Lett., 5* (1970) 337.
20 L. Ley, S. P. Kowalczyk, F. R. McFeely, R. A. Pollak and D. A. Shirley, *Phys. Rev. B, 8* (1973) 2392.
21 D. A. Shirley, *Chem. Phys. Lett., 16* (1972) 220.
22 D. W. Davis and D. A. Shirley, *Chem. Phys. Lett., 15* (1972) 185.
23 H.-J. Freund, E. W. Plummer, W. R. Salaneck and R. W. Bigelow, *J. Chem. Phys., 75* (1981) 4275.
24 H.-J. Freund, M. S. Banna, A. R. Slaughter, S. M. Ballina, R. W. Bigelow, B. Dick, J. Lex and H. Deger, *J. Chem. Phys., 81* (1984) 2535.
25 H.-J. Freund, W. Eberhardt, D. Heskett and E. W. Plummer, *Phys. Rev. Lett., 50* (1983) 768.
26 B. Johansson and N. Mårtensson, *Phys. Rev., 21* (1980) 4427.
27 D. Tomanek, P. A. Dowben and M. Grunze, *Surf. Sci., 126* (1983) 112.
28 C. D. Wagner, *Farad. Discuss. Chem. Soc., 60* (1975) 291.
29 C. D. Wagner, *J. Electron Spectrosc., 10* (1977) 305.
30 C. D. Wagner, *Surf. Sci., 35* (1973) 82.
31 C. D. Wagner, D. E. Passoja, H. F. Hillery, T. G. Kinsky, H. A. Six, W. T. Jansen and J. A. Taylor, *J. Vac. Sci. Technol., 21* (1982) 933.
32 G. Hohlneicher, H.-J. Freund and H. Pulm, *J. Electron Spectrosc.,* to be published.

33 R. Bicker, H. Deger, W. Herzog, K. Rieser, H. Pulm, G. Hohlneicher and H.-J. Freund, *J. Catal., 94* (1985) 69.
34 P. A. Anderson, *Phys. Rev., 54* (1938) 753.
35 M. Cardona and L. Ley (eds.), *Photoemission in Solids I + II,* Springer, Berlin, 1978.
36 J. C. Fuggle, *Surf. Sci., 69* (1977) 581.
37 C. D. Wagner and J. A. Taylor, *J. Electron Spectrosc., 20* (1980) 83.
38 A. A. Holscher, *Surf. Sci., 4* (1966) 89.
39 G. Johannsson, J. Hedmann, A. Berndtsson, M. Klasson and R. Nilson, *J. Electron Spectrosc., 2* (1973) 295.
40 K. D. Sevier, *Low Energy Electron Spectrometry,* Wiley-Interscience, New York, 1972.
41 D. E. Eastman, *Phys. Rev. B, 1* (1970) 1.
42 W. A. Coghlan and R. E. Clausing, *Atomic Data, 5* (1973) 317.
43 H. B. Michaelson, *J. Appl. Phys., 21* (1950) 536.
44 C. D. Wagner, *Anal. Chem., 47* (1975) 1201.
45 C. D. Wagner, *Anal. Chem., 44* (1972) 967.
46 O. Klein and E. Lange, *Z. Elektroch., 44* (1938) 558.
47 H.-J. Freund, H. Gonska and G. Hohlneicher, *J. Electron Spectrosc., 12* (1977) 425.
48 G. Carter and J. S. Colligon, *Ion Bombardment of Solids,* Heinemann, London, 1968.
49 M. S. Lazarus and T. K. Sham, *J. Electron Spectrosc., 31* (1983) 91.
50 E. E. Chaban and J. E. Rowe, *J. Electron Spectrosc., 9* (1976) 329.
51 R. J. Colton and J. W. Rabalais, *J. Electron Spectrosc., 7* (1975) 359.
52 J. H. Scofield, *J. Electron Spectrosc., 8* (1976) 129.
53 D. A. Shirley, *Photoemission in Solids, Vol. 1,* Springer, Berlin, 1978.
54 Polaschegg, Leybold-Heraeus SAV 2/75.
55 P. Ascarelli and G. Missioni, *J. Electron Spectrosc., 5* (1974) 417.
56 C. D. Wagner, *Anal. Chem., 51* (1979) 466.
57 R. P. Elliott, *Constitution of Binary Alloys, 1st Suppl.,* McGraw-Hill, New York, 1965.
58 M. Hansen and K. Anderko, *Constitution of Binary Alloys,* McGraw-Hill, New York, 1958.
59 G. Hohlneicher, *Ber. Bunsenges. Phys. Chem., 78* (1974) 1126.
60 A. Rosen and I. Lindgren, *Phys. Rev., 176* (1968) 114.
61 L. Hedin and A. Johansson, *J. Phys. B, 2* (1969) 1336.
62 M. E. Schwartz, *Chem. Phys. Lett., 6* (1971) 631.
63 G. K. Wertheim, R. L. Cohen, G. Crecelius, K. W. West and J. H. Wernick, *Phys. Rev. B, 20* (1979) 860.
64 J. B. Mann, *Los Alamos Scientific Lab. Rep. LASL-3690,* 1960.
65 R. E. Watson and M. L. Perlman, *Struct. Bonding, Berlin, 24* (1975).
66 K. Sham, R. E. Watson and M. L. Perlman, *Phys. Rev. B, 20* (1979) 3552.
67 A. N. Nethercot, Jr., *Phys. Rev. Lett., 33* (1974) 1088.
68 A. L. Allred and E. G. Rochow, *J. Inorg. Nucl. Chem., 5* (1958) 269.

Appendix A

Consider an Auger transition between an initial state with a hole in orbital j and a final state with two holes in orbital i. In the limit of complete relaxation [A1 - A3] the kinetic energy of the electron released by this process can be written as

$$E_{\mathrm{kin}}(jii, \mathrm{X}) = -\epsilon_j - R_j + 2\epsilon_i + R_{ii} - F(ii, \mathrm{X}) - \epsilon_{\mathrm{F}} \qquad \text{(A1)}$$

The ϵ are the orbital energies; R_j is the relaxation contribution to the single-hole initial state of the Auger process and R_{ii} the relaxation contribution of the double-hole final state; $F(ii, X)$ is the open shell interaction which determines a specific term X within the *jii* multiplet; ϵ_F is the Fermi energy of the sample. Combining eqn. (A1) with the expression for the corresponding binding energies

$$E_B(i) = -\epsilon_i - R_i + \epsilon_F \tag{A2a}$$

$$E_B(j) = -\epsilon_j - R_j + \epsilon_F \tag{A2b}$$

yields

$$2E_B(i) - E_B(j) + E_{kin}(jii, X) = -2R_i + R_{ii} - F(ii, X) \tag{A3}$$

In the case when the Auger multiplet does not change its structure but is shifted as a whole with variations in the chemical surrounding, we can consider the $F(ii, X)$ as constant and we obtain

$$2\,\Delta E_B(i) - \Delta E_B(j) + \Delta E_{kin}(jii) = 2\,\Delta R_i + \Delta R_{ii} \tag{A4}$$

Here ΔE_{kin} is the shift in the Auger multiplet which is now independent from X.

When the changes in the relaxation contribution are only due to coulomb forces the relaxation contribution for a state with two holes in the subshell *i* should be four times as large as the relaxation contribution for a state with a single hole in this shell [A4, A5]:

$$\Delta R_{ii} = 4\,\Delta R_i \tag{A5}$$

Insertion of eqn. (A5) into eqn. (A4) leads directly to eqn. (5). A detailed discussion of this derivation and the inherent approximations is given in ref. A6.

References for Appendix A

A1 W. N. Asaad and D. Petrini, *Proc. Phys. Soc. (London), 71* (1958) 369.
A2 D. A. Shirley, *Phys. Rev. A, 7* (1973) 1520.
A3 D. A. Shirley, *Chem. Phys. Lett., 17* (1972) 312.
A4 N. F. Mott and R. W. Gurney, *Electronic Processes in Ionic Crystals*, Oxford University Press, London, 1950.
A5 N. F. Mott and M. J. Littleton, *Trans. Farad. Soc., 34* (1938) 485.
A6 G. Hohlneicher, H.-J. Freund and H. Plum, *J. Electron. Spectrosc.*, to be published.